Catalysis Today 334 (2019) 122–130

Contents lists available at ScienceDirect

Catalysis Today

journal homepage: www.elsevier.com/locate/cattod

Selective catalytic oxidation over Au-Pd/titanate nanotubes and the influence of the catalyst preparation method on the activity

Motaz Khawaji, David Chadwick*

Department of Chemical Engineering, Imperial College London, London, SW7 2AZ, United Kingdom

ARTICLE INFO

Keywords:
Gold-palladium
Titanate nanotubes
Sol-immobilization
Graphene oxide
Selective oxidation

ABSTRACT

The dependence of the selective oxidation catalytic activity of Au-Pd supported on titanate nanotubes on the catalyst preparation method has been investigated. The most active Au-Pd/Ti-NT catalyst for the selective oxidation of benzyl alcohol is shown to be that prepared using colloidal synthesis and immobilization with PVA as a stabilizer, which has markedly superior catalytic activity compared to catalysts prepared by deposition-precipitation, adsorption, and dry impregnation methods. Au-Pd NPs stabilized by graphene oxide sheets and immobilized on Ti-NT has also been studied and while not optimum shows promising catalytic activity. The superior catalytic activity of the catalysts prepared by colloidal synthesis is attributed to the high metal dispersion on the external surfaces of Ti-NT, the narrow particle size distribution, and the high degree of Au-Pd alloying. This work also demonstrates that in the adsorption method of preparation using $HAuCl_4.3H_2O$ and $PdCl_2$ precursors, the uptake of Pd ions in solution by Ti-NT is proportional to the sodium content in Ti-NT, which implies that Na is involved in an ion-exchange reaction with Pd ions.

1. Introduction

The catalytic activity of gold is highly dependent on Au particle size and the dispersion of Au nanoparticles (NPs), both of which are influenced by the catalyst preparation method and the nature of the support. Usually, well-dispersed Au NPs of ≤ 5 nm in size display the highest catalytic activity [1,2], and it has been shown that different preparation methods produce different size distributions of Au NPs on the support [1,3]. A number of studies have shown that when Au NPs are dispersed on reducible metal oxides, especially TiO_2 and CeO_2, they exhibit high catalytic activity [4]. Therefore, optimum catalytic performance can be achieved by careful selection of the preparation method and support material.

The catalytic activity of gold is enhanced several fold by alloying gold with palladium [5]. In the selective oxidation of alcohols to aldehydes, for instance, alloying Au with Pd results in up to twenty-five-fold enhancement in the activity [1]. The synergy between Au and Pd has been attributed to the ability of Au atoms to draw electron density away from Pd atoms [1]. Gold and gold alloy catalysts have been prepared by a range of preparation methods including impregnation [6,7] deposition-precipitation, chemical vapor deposition [8], and sol-immobilization [9].

Titanate nanotubes (Ti-NT) possess unique physiochemical properties such as an open mesoporous structure, high specific surface area, high ion-exchange capacity for various metals, and good stability at moderately elevated temperatures [10]. These properties make Ti-NT a very attractive material for application in catalysis. A single nanotube is typically 50–200 nm in length and has an internal diameter ca. 3–8 nm, and an outer diameter ca. 8–15 nm [11]. While titania has been extensively and successfully used as a support material for Au and Au-Pd catalysts, especially for selective oxidation reactions [12,13], titanate nanotubes possess several advantages over conventional titania. For instance, titania (TiO_2 Aeroxide P25) has a surface area of $\sim 50\ m^2/g$ and surface hydroxyl group density $\sim 4.8\ -OH/nm^2$ [14], whereas Ti-NT have a surface area of $\sim 250\ m^2/g$ on average and surface hydroxyl density of $\sim 5.8\ -OH/nm^2$ [15]. In general, metal dispersion increases as the functionalities and surface area of the support increase [16]. In the present work, we investigate the use of Ti-NT as support for Au-Pd and show how the catalytic activity for selective oxidation is highly sensitive to the catalyst preparation method. The methods studied include sol-immobilization and adsorption, and for comparison two other common methods, namely deposition-precipitation, and dry impregnation. As part of this study, we have investigated in more detail the adsorption and ion-exchange processes involved in the preparation of Au-Pd catalysts by the adsorption method using $HAuCl_4.3H_2O$ and $PdCl_2$. We have also investigated the use of graphene oxide sheets

* Corresponding author.
E-mail address: d.chadwick@imperial.ac.uk (D. Chadwick).

https://doi.org/10.1016/j.cattod.2018.11.080
Received 2 July 2018; Received in revised form 3 November 2018; Accepted 30 November 2018
Available online 04 December 2018

instead of organic ligands in the stabilization of Au-Pd NPs. The present work establishes clearly that the catalytic activity of Au–Pd/Ti-NT is very dependent on the preparation method, the particle size, and the location of Au-Pd NPs and their dispersion on the surface of Ti-NTs and that sol-immobilization is the more effective method of preparation.

2. Materials and methods

2.1. Materials

All metal precursors and chemical reagents were purchased from Sigma Aldrich and used as received: NaOH (99.99% trace metals basis), H_2SO_4(≥97.5% purity), TiO_2 (Aeroxide® P25), poly(vinyl alcohol) (PVA) (Mw 9,000–10,000, 80% hydrolysed), $HAuCl_4.3H_2O$ (99.999% purity), $PdCl_2$ (5 wt. % in 10 wt. % HCl), $NaBH_4$ (Aldrich ≥98.0%), Palladium(II) acetate (≥99.9% purity), Benzyl alcohol (99.8% purity). O_2 (100% pure) for catalytic tests was supplied by BOC.

2.2. Catalyst preparation

2.2.1. Synthesis of titanate nanotubes (Ti-NTs)

Titanate Nanotubes (Ti-NTs) were synthesized by the alkaline hydrothermal treatment method as reported by Kasuga et al. [17]. In a typical synthesis, 11.0 g of TiO_2 was added to 185 mL of 10 M NaOH in a 200 mL PTFE-liner and stirred for two hours. The PTFE-lined steel autoclave was then placed in an air-circulating oven at 140 °C for 24 h. The obtained slurry was then washed with DI water, filtered and dried overnight at 120 °C. The dried powder was washed with 0.1 M H_2SO_4 and filtered. This process was repeated until pH 7 was reached. Finally, the Ti-NTs powder was washed thoroughly with DI water to remove any residual H_2SO_4, and dried overnight at 120 °C.

2.2.2. Catalysts prepared by dry Impregnation (Au-Pd/Ti-NT^{DI})

The requisite amounts of gold precursor ($HAuCl_4.3H_2O$) and palladium precursor ($PdCl_2$, 5 wt.% in HCl) were dissolved in a predetermined volume of DI water to give a surface loading of ~200,000 m^2/L. The precursor solution was added drop-wise to the support to form a fine paste. The paste was dried overnight at 120 °C, and then reduced for 2 h at 200 °C in a tube furnace under a continuous flow of diluted hydrogen (5 vol.% H_2 /Ar). The furnace ramp rate was set to 5 °C/min, and gas flow rate was fixed at ~50 mL/min.

2.2.3. Catalysts prepared by adsorption (Au-Pd/Ti-NT^{ADS})

The required amounts of ($HAuCl_4.3H_2O$) and ($PdCl_2$, 5 wt.% in HCl) corresponding to the desired loadings were added to 100 mL of DI water at 80 °C. Under vigorous stirring conditions, 1.0 g of the support was added to the solution. After 18 h, the solution was filtered and dried overnight at 120 °C. The catalyst was reduced in H_2 as described in the previous section.

2.2.4. Catalysts prepared by deposition-precipitation (Au-Pd/Ti-NT^{DP})

Typically, 1.0 g of the support was added to 75 mL of DI water at 80 °C. Aqueous solutions of $HAuCl_4$ (2 mM) and palladium(II) acetate (2 mM) were prepared and used as the metal precursors. The required volumes of the aqueous solutions corresponding to the final desired loading were added to the support. The deposition-precipitation was performed using Metrohm 902 Titrando auto-titrator. The pH was maintained at 8 by continuous dosing of NaOH (0.1 mM). The solution was left stirring for 16 h before being filtered and washed with 1 L of DI water. The catalyst was subsequently dried at 120 °C and reduced under the same reduction conditions previously described.

2.2.5. Catalysts prepared by sol-immobilisation (Au-Pd/Ti-NT^{SI-PVA})

Catalysts were prepared in manner similar to the sol-immobilization procedure reported previously [18]. First, Ti-NT were acidified to a pH below the point of zero charge (PZC). Typically, 1.0 g of the support was added to 75 mL of water and a 1.0 M solution of H_2SO_4 was added drop-wise to the slurry until the pH dropped to ~1.5. After 2 h of vigorous stirring, the slurry was filtered and the acidified support was collected and added to the metal sol.

The metal sol was prepared by adding predetermined amounts of the gold precursor ($HAuCl_4.3H_2O$) and palladium precursor ($PdCl_2$, 5 wt.% in HCl) to 100 mL of DI water while stirring vigorously. Subsequently, a specified amount of the stabilizer PVA (1.0 wt.% solution) was added to the solution and stirred for 15 min. The weight ratio was PVA/(Au + Pd) = 1.2. The metal precursors were reduced in-situ by the addition of an excess amount of $NaBH_4$ such that the molar ratio of $NaBH_4$:(Au + Pd) was 5:1. The sol was left stirring for 1 h before the acidified Ti-NTs were added to form a slurry. The slurry was left stirring for 2 h before it was filtered and washed with DI water several times until the pH of the mother liquor reached ~7.0. The obtained catalyst was finally dried overnight at 120 °C. Catalyst Au-Pd/Ti-NT^{SI-PVA} was refluxed in hot water (90 °C) for 60 min, filtered and dried overnight at 120 °C.

2.2.6. Preparation using graphene oxide (Au-Pd/Ti-NT^{GO})

Catalyst was prepared as for the sol-immobilized catalyst above except that GO dispersed in water (0.5 mg/mL) was added to the solution instead of PVA. The weight ratio was GO/(Au + Pd) = 1.5. For the GO stabilized catalyst the hot water reflux was not carried out.

2.3. Reaction procedure

Benzyl alcohol oxidation was carried out in a batch reactor using 25 mL glass-lined minclaves (Buchiglas, Switerland). In a typical run, benzyl alcohol (2.50 g) and the required amount of catalyst were charged to the reactor before it was purged five times with O_2. Subsequently, the reactor was pressurized with O_2 to the required pressure at room temperature. The reactor was heated in an oil bath set at the desired temperature and stirred at 1000 rpm. An oxygen tank was connected to the reactor to guarantee that any oxygen consumed by the reaction was replenished. At the end of each run, the reactor was cooled down to room temperature and vented slowly. The reaction mixture was dissolved in 20 mL of acetonitrile and then centrifuged at 5000 rpm for 15 min to separate out the catalyst. A sample from the supernatant (600 µL) was taken out and added to 100 µL of n-butanol (internal standard) prior to product analysis with GC. Analysis of the reaction products was carried out using a GC (Shimadzu GC-2014) fitted with a Flame Ionization Detector (FID), and a wax column (Agilent CP WAX 52 CB UltiMetal, L = 25 m, ID = 0.53 mm, film thinness = 2.0 µm). Carbon balance was 96 ± 3%. Benzyl alcohol (BA) conversion (X_{BA}), product yield (Y_i), and selectivity (S_i) were calculated using the following equations:

$$Y_i\,(wt.\%) = \frac{w_i}{w^{\circ}_{BA}} \times 100\%$$

$$X_{BA}\,(wt.\ \%) = \sum_{i=1}^{n} Y_i$$

$$S_i\,(wt.\%) = \frac{w_i}{\sum_{i=1}^{n} w_i} \times 100\%$$

Where: w°_{BA} is the initial amount of benzyl alcohol, and w_i is the final amount of carbon containing product i.

2.4. Catalyst characterisation

Catalysts were analyzed by PANalytical X'Pert Pro Multi-Purpose Diffractometer using Cu-Kα radiation. The analysis was performed over a scan angle of 5-70° 2θ, and a step size of 0.0167°. Nitrogen adsorption-desorption measurements were carried out at −196 °C using a Micromeritics TriStar II. Prior to carrying out any measurements,

samples were degassed at 140 °C for 12 h. Brunauer–Emmett–Teller (BET) and Barrett-Joyner-Halenda (BJH) were used to measure the specific surface area (S_{BET}), pore volume and pore diameter. The bulk metal loading was determined by inductively coupled plasma atomic emission spectroscopy (ICP-AES, PE Optima 2000 DV). Typically, 10–12 mg of catalyst was dissolved in 15 mL of aqua regia, sonicated for 2 h, and diluted with 20 mL of DI water. The instrument was calibrated with authenticated standards (Sigma Aldrich) containing predetermined amounts of each metal.

The particle size distributions of the metal NPs were determined from high resolution transmission electron microscopy (HRTEM) images. HRTEM images were collected using a JEOL JEM-2100 F microscope operating at 200 kV. Samples were dispersed in ethanol and sonicated for 30 min before they were placed on copper grids with a holey carbon film (300 mesh size).

X-ray photoelectron spectroscopy (XPS) measurements were recorded using a Thermo K-Alpha Spectrometer equipped with Al Kα source gun. Samples were mounted on double-sided adhesive tape, and the spectra were collected using an X-ray spot size of 400 µm with a pass energy of 20 eV with 0.1 eV increments. The binding energies (BE) were referenced to the C(1 s) peak of adventitious carbon at 284.8 eV. Data analysis and peak fitting were performed using Avantage software provided by Thermo Scientific. The error in the XPS measurement is typically ± 0.2 eV.

The point of zero charge (PZC) for the as-synthesized Ti-NT was determined by measuring the zeta potential of Ti-NTs as a function of pH using Brookhaven ZetaPALS Potential Analyzer. Ti-NT were dispersed in diluted solutions of KOH and HNO_3 at varying pH values ranging from 2 to 11.

3. Results and discussion

As noted in the Introduction above, titanate nanotubes possess several advantages over conventional titania as a support for Au and Au-Pd. Ti-NT has a high surface area ~250 m^2/g on average and high surface hydroxyl density ~5.8 −OH/nm [15]. Since, in general, the metal dispersion increases as the functionalities and surface area of the support increase [16], these are attractive features that can be leveraged by suitable catalyst preparation. First, we describe the synthesis and characterization of the Ti-NT support.

3.1. Synthesis of Ti-NT

Ti-NTs were prepared by alkaline hydrothermal treatment as reported by Kasuga et al. [17]. The synthesis of Ti-NT by alkaline hydrothermal treatment leads to the formation of layered nanostructured sodium titanate ($Na_2Ti_3O_7$, JCPDS No. 31-1329), in which sodium atoms are located on the surface and in the interlayer spacing of the nanotubes [19,20]. Acid treatment of the sodium form of titanate nanotubes result in an ion-exchange process whereby Na^+ cations are replaced with protons (H^+). Once the ion-exchange process is completed, the hydrogen/protonated form of titanate nanotubes ($H_2Ti_3O_7$, JCPDS No. 41-192) is produced [11]. In this study, two forms of Ti-NT were prepared and used as catalyst supports: one set which contained some residual sodium (Na = 5.27 wt.%) and was designated as Ti-NT-1, and a second set which was treated several times with 0.1 M sulphuric acid to achieve minimum sodium content (< 200 ppm), and denoted as Ti-NT-2, which is considered to be essentially Na free. Generally, the formation of Ti-NT is characterized by the emergence of a broad angle peak between 7.2 and 10.3° 2θ in the XRD pattern [21], as shown in Fig. 1a. This low angle peak has been ascribed to the interlayer spacing of the layered titanate phase. The peaks at 24.5°, 28.6° and 48.6° for Ti-NT-1 and Ti-NT-2 are attributed to tri-titanate 1D nanomaterials [22]. The weakening of the peak at ca. 2θ = 28.6°, and the broadening of the peak at 2θ = 10.3° in Ti-NT-2 is a result of the removal of Na and proton exchange [23]. The disappearance of the characteristic anatase peaks also confirmed the transformation of the starting material into titanate. The formation of Ti-NT was also confirmed by TEM (Fig. 1b), where the multi-walled tubular structure of the Ti-NT is clearly seen.

3.2. Catalyst preparation

This section discusses features of the different catalyst preparation methods investigated. All the catalysts have been prepared to have a nominal metal loading of 2.0 wt.% with a Au:Pd weight ratio equal to 1.0 (Au:Pd atomic ratio = 1:1.86). Table 1 lists the metal contents for the various supports and catalysts. The titanate nanotube support essentially sodium free (Ti-NT-2) was used in the preparation of catalysts Au-Pd/Ti-NT^{SI-PVA}, Au-Pd/Ti-NT^{GO}, Au-Pd/Ti-NT^{DP}, and Au-Pd/Ti-NT^{DI}. Ti-NT-1 containing residual sodium (5.27%) was used only for the preparation of catalyst Au-Pd/Ti-NT^{ADS} as discussed below.

3.2.1. Adsorption

We have previously prepared highly active Au-Pd/Ti-NT catalysts using an adsorption method [13]. However, we found that the effective preparation of Au-Pd/Ti-NT by this method using $HAuCl_4.3H_2O$ and $PdCl_2$ depends on many factors such the sodium content in Ti-NT, the metal precursors and their concentration, and the pH of the solution. This prompted us to investigate this process in more detail, and conclude that preparation of Au-Pd/Ti-NT catalysts using the adsorption method and readily available chloride precursors (i.e. $HAuCl_4.3H_2O$ and $PdCl_2$) in fact involves two processes: adsorption and ion-exchange.

During catalyst preparation, solid hydrogen tetrachloroaurate(III) hydrate was dissolved in DI water, and hydrolyzed to form an anionic Au complex (i.e. $AuCl_4^-$). The internal and external surfaces of Ti-NT possess an abundance of hydroxyl groups (−OH) which can be protonated ($-OH_2^+$) or deprotonated ($-O^-$) depending on the pH of the aqueous suspension [13]. The zeta potential of a Ti-NT-2 suspension was measured at different pH values, and the PZC was found to be ca. 5.2 as shown in Fig. 2. When the pH of the solution was lower than the PZC of Ti-NT, the anionic Au complex was efficiently adsorbed by Ti-NT, and high Au loading was obtained. Furthermore, it was also observed that the adsorption of the Au complex was dependent on the concentration of the Au precursor and the Cl^- anions present in the solution (entries 1–6 in Table 1). When the concentration of Cl^- anions was high, very low Au loading was achieved, which suggests that Cl^- ions can competitively adsorb on the support and block the adsorption sites available for the $AuCl_4^-$ complex. In fact, this observation is in agreement with previous studies in which a high concentration of Cl^- ions was found to suppress $AuCl_4^-$ adsorption on alumina [24,25].

On the other hand, the loading of Pd on Ti-NT was found to be proportional to the amount of Na present in Ti-NT. When Ti-NT were almost fully protonated (entry 1 in Table 2), minimal Pd loading was achieved. As the sodium content in Ti-NT increased, a higher loading of Pd was obtained (entries 1–4 in Table 2). These results indicate that Pd ions were taking part in an ion-exchange reaction with Na in Ti-NT, while the protons were not found to be easily exchangeable with Pd ions. A similar observation has been made previously by Song et al. [26] with lead cations, where it was found that sodium ions in Ti-NT were exchangeable with lead ions, while protons were not. The difference in the ion-exchange capacity of sodium titanate nanotubes in comparison with protonated titanate nanotubes has been ascribed to the layer space effect of nanotubes [11,26]. The d-value of the interlayer spacing of sodium titanate nanotubes has been shown to be larger than protonated titanate nanotubes [27,28]. The catalyst with the highest actual Au-Pd loading (entry 6) was used for the catalytic test and is denoted as Au-Pd/Ti-NT^{ADS} throughout.

Although a very active catalyst with high metal dispersion is produced with this method of preparation [13], the reproducibly of the catalyst can be challenging. This is due to the two complex and simultaneous physiochemical processes (i.e. ion-exchange and adsorption) which are very sensitive to the preparation conditions and the

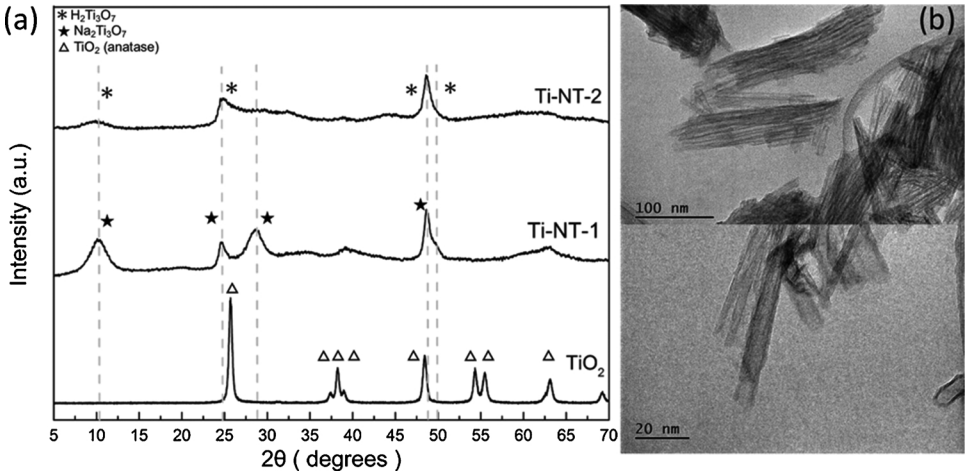

Fig. 1. (a) XRD patterns for starting TiO_2 powder, Ti-NT-1 (containing residual sodium) and Ti-NT-2 (sodium-free). Patterns were indexed using TiO_2 (JCPDS No. 21-1272), $Na_2Ti_3O_7$ (JCPDS No. 31-1329) and $H_2Ti_3O_7$ (JCPDS No. 41-192), (b) TEM images of as synthesized Ti-NT-2.

Table 1
Au, Pd and Na content in the Au-Pd/Ti-NT and the as-synthesized Ti-NT supports.

Sample	Metal content[a] (wt.%)		
	Au	Pd	Na
Ti-NT-1	–	–	5.27
Ti-NT-2	–	–	0.02
Au-Pd/Ti-NT^{ADS}	0.64	0.88	2.37
Au-Pd/Ti-NT^{SI-PVA}	0.70	0.77	trace
Au-Pd/Ti-NT^{GO}	0.81	0.82	trace
Au-Pd/Ti-NT^{DP}	0.79	1.10	trace
Au-Pd/Ti-NT^{DI}	0.84	1.15	trace

[a] Weight percentage per gram of sample, obtained by ICP-AES analysis.

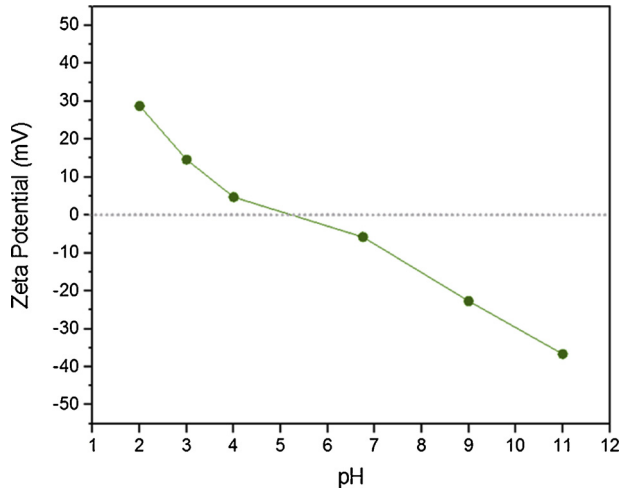

Fig. 2. Zeta potential measurement for as-synthesized Ti-NT-2 as a function of pH.

starting sodium content in the Ti-NT. Furthermore, the presence of significant residual sodium in the final catalyst is problematic because it can have an impact on the catalytic performance. Therefore, an alternative preparation method for Au-Pd/Ti-NT catalysts that is reproducible and does not depend on the starting sodium content, and provides a sodium-free catalyst is highly desirable.

3.2.2. Sol-immobilization and catalysts stabilized with GO

The Au-Pd colloids were prepared as described in the experimental section above. Au-Pd sols are typically stabilized by organic surfactants such as polyvinylpyrrolidone (PVP) and poly(vinyl alcohol) (PVA) [29,16]. Catalysts prepared by sol-immobilization using polymer ligands have been shown to give active Au-Pd catalysts on conventional oxide supports [18], and carbon [30]. We have previously used sol-immobilization with PVA to prepare highly active Au-Pd/Ti-NT catalysts [13], and have shown the resultant catalyst to be more active than the equivalent catalyst supported on commercial TiO_2 nanopowders [31].

Table 2
Effect of sodium content in Ti-NT on the uptake of the metal precursors (pH < PZC).

Entry	Na (wt.%)		Pd (wt.%)		Au (wt.%)		Cl^- level
	Initial	Final	Nominal	Actual	Nominal	Actual	
1	0.02	0.01	1.00	0	1.00	0	high [Cl^-]
2	0.39	0.08	1.00	0.03	1.00	0	high [Cl^-]
3	1.66	0.67	1.00	0.25	1.00	0	high [Cl^-]
4	5.27	2.92	1.00	0.91	1.00	0.03	high [Cl^-]
5	2.15	0.01	1.00	0.73	1.00	0.68	low [Cl^-]
6	5.27	2.37	1.00	0.88	1.00	0.64	low [Cl^-]

Two-dimensional graphene oxide (GO) is amphiphilic with surfactant-like properties. It contains both hydrophilic groups (i.e. hydroxyl and carboxyl) and un-oxidized hydrophobic polyaromatic nanographene domains [32,33]. Recently, Hutchings and co-workers used 2D GO sheets to stabilize Au-Pd NPs [34]. The GO-stabilized NPs were subsequently immobilized on conventional TiO_2 nanopowders to create a ternary hybrid catalyst (Au-Pd-GO/TiO_2). The catalytic activity of this new catalyst was tested in the selective oxidation of benzyl alcohol and displayed a comparable activity to the PVA-stabilized catalysts (Au-Pd-PVA/TiO_2), and enhanced stability. This novel strategy is very attractive because it avoids the use of organic ligands, which are susceptible to decomposition under reaction conditions. In this study, we have adopted this unconventional strategy to prepare a new catalysts where Au-Pd NPs are stabilized by GO sheets and supported on Ti-NT. This catalyst is denoted as Au-PdTi-NT^{GO}, while the catalyst prepared using sol-immobilization with PVA is denoted as Au-Pd/Ti-NT^{SI-PVA}.

3.2.3. Dry impregnation and deposition-precipitation

For comparison purposes, Au-Pd/Ti-NT catalysts were prepared by conventional dry impregnation and deposition-precipitation. Catalyst samples Au-Pd/Ti-NT^{ADS}, Au-Pd/Ti-NT^{DP}, Au-Pd/Ti-NT^{DI} were reduced with molecular hydrogen at a relatively moderate temperature (i.e. 200 °C) to avoid sintering of Au-Pd NPs, and damaging the structure of

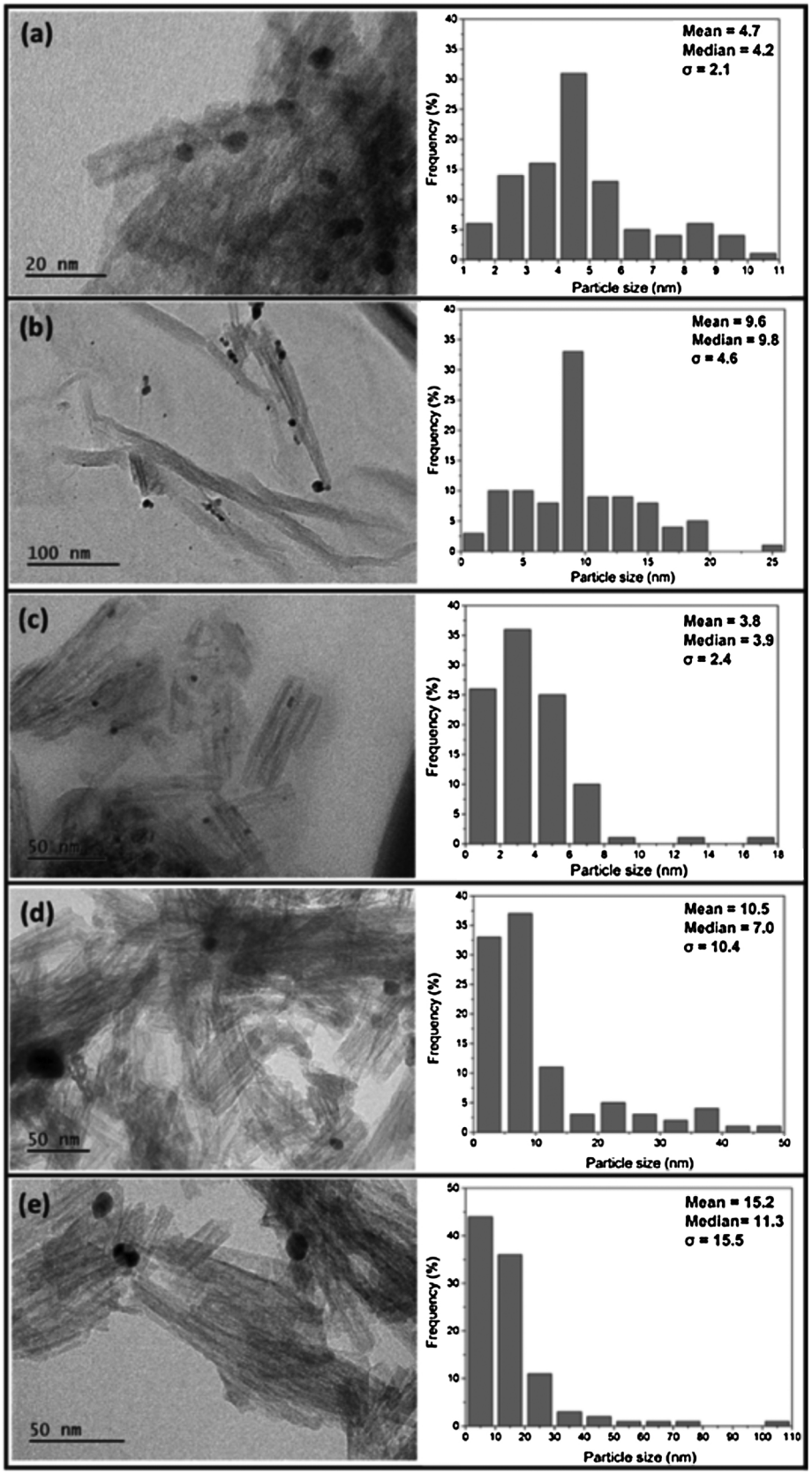

Fig. 3. TEM images and the corresponding particle size distribution for (a) Au-Pd/Ti-NT^{SI-PVA}, (b) Au-Pd/Ti-NT^{GO}, (c) Au-Pd/Ti-NT^{ADS}, (d) Au-Pd/Ti-NT^{DP} and (e) Au-Pd/Ti-NT^{DI}.

Table 3
XPS and bulk atomic ratios, metal particle size and dispersion for the various catalysts.

Catalyst	Pd/Au atomic ratio[a]		(Au + Pd)/Ti[a]	Mean particle size (nm)[b]	Metal dispersion (%)[b]
	ICP	XPS			
Au-Pd/Ti-NT^{SI-PVA}	2.04	2.20	0.19	4.7 ± 2.1	31
Au-Pd/Ti-NT^{GO}	1.86	1.85	0.12	9.7 ± 4.6	18
Au-Pd/Ti-NT^{ADS}	2.55	2.42	0.01	3.8 ± 2.4	40
Au-Pd/Ti-NT^{DP}	2.57	4.00	0.02	10.5 ± 10.4	24
Au-Pd/Ti-NT^{DI}	2.53	3.38	0.02	15.2 ± 15.5	14

[a] Determined from XPS.
[b] Determined from TEM images.

Ti-NT. It was previously shown that reduction of the metal precursors under these condition is sufficient, and produces active catalysts [12,35].

3.3. Catalyst characterization

3.3.1. TEM

TEM images revealed information pertaining to the morphology and structure of the various catalysts, and particle size distribution (PSD) of Au-Pd NPs on the surface of Ti-NT (Fig. 3). The catalysts displayed very different PSD and mean particle sizes. Catalyst sample Au-Pd/Ti-NT^{ADS} exhibited the narrowest PSD and smallest mean particle size (Fig. 3.c). Notably, the catalyst stabilized with GO sheets (Fig. 3.b) exhibited a larger mean particle size and wider distribution than the catalyst sample stabilized by PVA (Fgure 3.a). Deposition-precipitation gave a relatively small mean particle size and a wide PSD (Fig. 3.d), while dry impregnation resulted in a very wide PSD and large mean particle size, with occasional particles as large as 100 nm.

The metal dispersion (%) was calculated using particle size distributions from the TEM images (Fig. 3) and the approximation method reported by Mori et al. [36], Table 3. Metal NPs were assumed to be face-centered cubic (FCC) cub-octahedral in shape. The highest metal dispersion (ca. 40%) was displayed by Au-Pd/Ti-NT^{ADS} due to its small mean particle size, followed by Au-Pd/Ti-NT^{SI-PVA}, and Au-Pd/Ti-NT^{GO}. The catalyst sample prepared by conventional dry impregnation (Au-Pd/Ti-NT^{DI}) displayed the lowest metal dispersion.

3.3.2. XRD

The XRD patterns of the catalysts are shown in Fig. 4 with detailed scan of the Au(111) region inset. Catalysts Au-Pd/Ti-NT^{ADS}, Au-Pd/Ti-NT^{DI} and Au-Pd/Ti-NT^{DP} displayed relatively sharp peaks close to the reflection of the pure Au(111) plane at ~38.41°. In contrast, catalysts Au-Pd/Ti-NT^{SI-PVA} and Au-Pd/Ti-NT^{GO} displayed Au(111) peaks at higher 2θ. The shift in the X-ray diffraction peak is a result of the change in the lattice constant from formation of a Pd-Au alloy phase [37]. No other clear diffraction peaks corresponding to the Au or Pd diffraction planes were observed in any of the catalysts owing to the low metal concentration and relatively small particle size of the metal NPs.

3.3.3. XPS

The surface chemistry and atomic composition of Au-Pd on the surface of the Ti-NT support were investigated by XPS. The XPS Au 4f spectra of the various catalysts are shown. It can be clearly observed that for some catalysts, the Au 4f binding energies (B.E.) are slightly lower than what is frequently observed for metallic gold. For a pure metallic gold film, a binding energy of ca. 84.0 eV is often observed for the Au ($4d_{7/2}$) component. In XPS, the exact location of the peaks is sensitive to factors such as the chemical environment and the metal–support interaction. For Au NPs deposited on Ti-NT, the Au ($4d_{7/2}$)

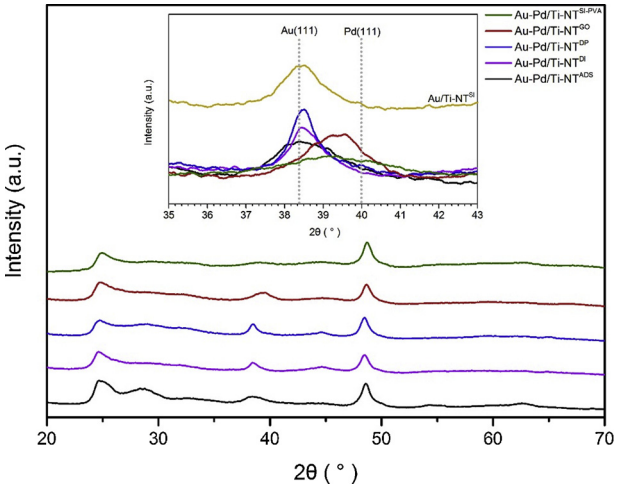

Fig. 4. X-ray diffraction patterns for the various Au-Pd/Ti-NT catalysts prepared in the study. Inset shows the shift of the Au(111) diffraction peak due to alloy formation.

binding energy has been shown to be at ca. 83.6 eV [31]. Catalyst samples Au-Pd/Ti-NT^{SI-PVA} and Au-Pd/Ti-NT^{SI-GO} exhibited the largest negative shift in the B.E. as shown in Fig. 4. In comparison Au-Pd/Ti-NT^{ADS} and Au-Pd/Ti-NT^{DI} exhibited peaks with binding energies closer to that observed for monometallic Au NPs supported on Ti-NT, while Au-Pd/Ti-NT^{DP} displayed a very small B.E. shift. The negative peak shift is ascribed to the electronic modification of Au species by Pd, and is indicative of a close interaction between the Au and Pd atoms, and formation of Au-Pd alloys [38]. Recent consensus in literature attribute the B.E. shift to a net charge transfer from Pd to Au and orbital rehybridization of both metals [38–40].

The corresponding Pd 3d spectra for the various catalysts are shown in Fig. 5b. The binding energy for Pd^0 usually falls between ca. 334.5 and 336.2 eV, whereas PdO_y species appear at higher binding energies, typically between 336.4 and 338.7 eV [31–41]. The Pd 3d XPS spectra of catalysts Au-Pd/Ti-NT^{SI-PVA}, Au-Pd/Ti-NT^{GO} and Au-Pd/Ti-NT^{DP} exhibit mostly Pd^0, indicative of Au-Pd alloying. On the other hand, catalyst samples Au-Pd/Ti-NT^{DI} and Au-Pd/Ti-NT^{ADS} show the presence of a high surface concentration of oxidized palladium species. Metallic Pd NPs are known to be susceptible to oxidation upon exposure to air such as occurs during the drying and transfer of the samples.

Therefore, the XPS results imply that Au-Pd NPs are present mostly as bimetallic alloys in catalyst samples Au-Pd/Ti-NT^{SI-PVA}, and Au-Pd/Ti-NT^{GO} and to a lesser extent in Au-Pd/Ti-NT^{DP}. The absence of a noticeable Au 4f binding energy shift and the high level of Pd surface oxidation for catalysts Au-Pd/Ti-NT^{ADS} and Au-Pd/Ti-NT^{DI} suggest a low level of alloy formation in these catalysts and implies that these preparation methods do not lead to significant alloy formation. Indeed, these results are consistent with our previous STEM-EDX spot analysis and elemental mapping of Au-Pd NPs prepared by sol-immobilization and adsorption in which Au-Pd NPs prepared by sol-immobilization were found to be predominantly homogenous mixed random alloys, whereas the Au and Pd NPs found in Au-Pd/Ti-NT^{ADS} were primarily monometallic in nature [13]. These results are also consistent with the existence of separate processes for the deposition of Au and Pd during the preparation of Au-Pd/Ti-NT^{ADS}.

From the fitted XPS data, the atomic surface composition of Au and Pd was estimated for the various catalysts. Table 3 shows the atomic of (Au + Pd)/Ti and Pd/Au. The evidently high (Au + Pd)/Ti ratio observed for Au-Pd/Ti-NT^{SI-PVA} and Au-Pd/Ti-NT^{GO} indicates high metal surface concentration and high metal dispersion. In comparison, the catalysts prepared by adsorption, deposition-precipitation and dry impregnation exhibited low Au and Pd surface concentrations, which can be attributed to either the poor dispersion of large Au-Pd NPs, and/or

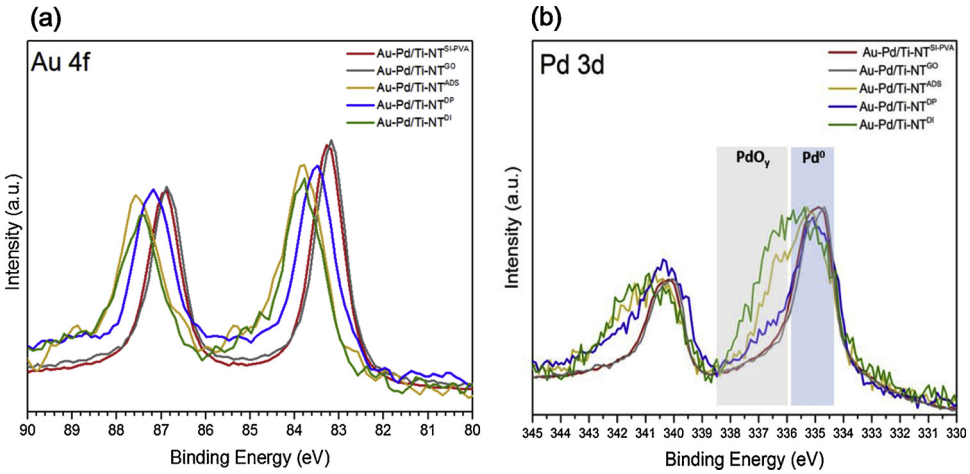

Fig. 5. XPS spectra of (a) Au 4f and (b) Pd 3d for the Au-Pd/Ti-NT catalysts.

the confinement of some small metal NPs (< 5 nm) inside the tubular structure of Ti-NT, which has been shown to be the case for Au-Pd/Ti-NT^{ADS} [13].

For Au-Pd/Ti-NT^{SI-PVA} and Au-Pd/Ti-NT^{GO}, the Pd/Au ratio derived from XPS was found to be reasonably close to the bulk ratio, which implies uniform and homogenous metal dispersion. The slight discrepancy between the two ratios likely reflects the difference in the XPS analysis depth between Au and Pd, and might imply different degree of surface enrichment in the bimetallic Au-Pd NPs. The discrepancy between the bulk and XPS ratios was considerably large for the catalyst prepared by deposition-precipitation which points to surface enrichment in Pd and/or the presence of some unalloyed Pd NPs.

3.4. Catalytic performance

The solvent-less selective oxidation of benzyl alcohol to benzaldehyde has been used extensively as a model oxidation reaction for studying Au-Pd supported catalysts [1,9,40,41]. The two primary products in the selective oxidation of benzyl alcohol are benzaldehyde and toluene. Other by-products such benzene, benzoic acid and benzyl benzoate can also be produced during the reaction. Benzaldehyde is formed by the sequential oxidative dehydrogenation of benzyl alcohol, while toluene is produced as a result of the disproportionation of benzyl alcohol [42,43].

We investigated the catalytic performance of the various Au-Pd/Ti-NT catalysts, and examined the influence of the catalyst preparation method on the activity and selectivity. All the catalysts were tested under the same reaction conditions (T = 120 °C, PO_2 = 4 bar, stirring rate = 1000 rpm, reaction time = 1 h). Fig. 6 shows the turnover frequency (TOF_{bulk}) displayed by the various catalysts, and Table 4 gives the benzyl alcohol conversion and product selectivity. In the absence of a catalyst, a benzyl alcohol conversion of ca. 4.4 wt.% was obtained due to the autoxidation of benzyl alcohol with molecular oxygen. The catalyst preparation method had a strong influence on the catalytic activity and selectivity, with sol-immobilization producing the most active catalyst.

Despite the differences in conversion, the product selectivity (Table 4) appeared to be influenced by the catalyst preparation method with Au-Pd/Ti-NT^{DP} exhibiting the lowest selectivity towards toluene and as a consequence the highest selectivity towards benzaldehyde. Notwithstanding possible differences in NP surface compositions, selectivity to toluene is probably associated with differences in surface acidity and surface impurities. Particularly, in the preparation of Au-Pd/Ti-NT^{DP}, palladium (II) acetate was used as a precursor and sodium hydroxide as the precipitating agent. Careful examination of the Na and Cl regions of the XPS, showed that the surface of Au-Pd/Ti-NT^{DP}

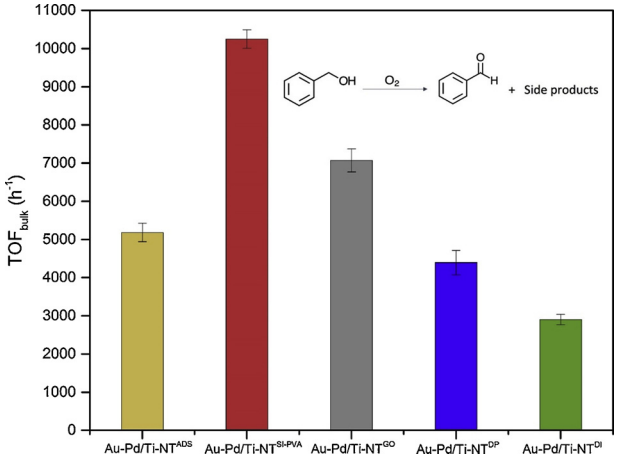

Fig. 6. Turnover frequency (TOF_{bulk}) determined for the different catalysts on the basis the bulk metal content.

contained retained Na, even though only traces were detected in the bulk analysis. Catalyst Au-Pd/Ti-NT^{ADS} which contained residual Na (see Table 1) displayed the second lowest selectivity to toluene and also the second highest selectivity to benzaldehyde. In this case XPS confirmed the presence of surface Na. Au-Pd/Ti-NT^{DI} presented the highest selectivity to toluene even though the conversion was low, and XPS detected significant surface Cl. XPS did not detect surface Na or Cl in catalysts Au-Pd/Ti-NT^{SI-PVA} or Au-Pd/Ti-NT^{GO}. Higher surface acidity appears to promote the disproportion of benzyl alcohol to toluene and benzaldehyde, while conversely lower surface acidity seems to mitigate it. A similar observation has been made by others [42,43].

Since the Au-Pd dispersion is quite different in the various catalysts, the TOF was also calculated on the basis of the number of surface Au and Pd atoms estimated using the metal dispersion calculated using the particle size distribution from TEM (see Table 4). Table 5 gives a comparison between the turnover frequency calculated on the basis of bulk metal loading (TOF_{bulk}) and the one calculated on the basis of surface metals ($TOF_{surface}$). The interpretation of $TOF_{surface}$ remains somewhat speculative. However, the comparison between bulk and surface values for the various catalysts reveals some interesting features. For example, the low $TOF_{surface}$ for catalyst Au-Pd/Ti-NT^{ADS} suggests that a large number of the highly-dispersed NPs are not participating in the catalytic reaction, most likely because they are not easily accessible. This result is in agreement with the TEM and XPS analysis and strongly supports our previous conclusion regarding the confinement of some small metal NPs inside the tubular structure and

Table 4
Benzyl alcohol conversion and product selectivity for the different catalysts.[a].

Catalyst	Conversion (%)	Product selectivity (wt.%)					
		Benzaldehyde	Toluene	Benzene	Benzyl ether	Benzoic acid	Benzyl benzoate
–	4.4	87.2	2.3	10.5	0	0	0
Au-Pd/Ti-NT^{SI-PVA}	84.1	77.8	9.4	1.6	4.2	1.4	5.7
Au-Pd/Ti-NT^{GO}	70.0	82.6	7.6	1.5	2.0	1.8	4.6
Au-Pd/Ti-NT^{ADS}	57.1	84.7	6.6	1.5	2.0	1.3	4.0
Au-Pd/Ti-NT^{DP}	45.5	92.0	0.6	1.6	0	1.7	4.0
Au-Pd/Ti-NT^{DI}	34.4	79.0	13.2	1.4	1.9	1.4	3.1

[a] Reaction conditions: T = 120 °C, P_{O2} = 4 bar, stirring rate = 1000 rpm, reaction time = 1 h, catalyst = 18 mg, benzyl alcohol = 2.5 g.

Table 5
Comparison between the TOF_{bulk} and $TOF_{surface}$ for the various catalysts.

Catalyst	TOF_{bulk}[a] (h^{-1})	$TOF_{surface}$[b] (h^{-1})
Au-Pd/Ti-NT^{SI-PVA}	10,250	32,932
Au-Pd/Ti-NT^{GO}	7,071	39,923
Au-Pd/Ti-NT^{ADS}	5,181	13,047
Au-Pd/Ti-NT^{DP}	4,391	18,409
Au-Pd/Ti-NT^{DI}	2,901	20,366

[a] Moles of benzyl alcohol converted per mole of metals (ICP-AES) per hour.
[b] Moles of benzyl alcohol converted per mole of surface metals (TEM) per hour.

interstitial cavities of Ti-NT. Interestingly, the $TOF_{surface}$ for catalyst Au-Pd/Ti-NT^{GO} was remarkably high. The observed enhancement in the activity of surface atoms for this catalyst over Au-Pd/Ti-NT^{SI-PVA} is likely due to the GO. It is highly plausible for GO sheets to interface with Au-Pd NPs and Ti-NT and enhance the catalytic activity and selectivity by altering the electronic properties of the catalyst and/or facilitating the diffusion and activation of the reactants. Nonetheless, this aspect needs further investigation.

The high $TOF_{surface}$ of catalysts Au-Pd/Ti-NT^{SI-PVA} and Au-Pd/Ti-NT^{GO} is a result of the high degree of alloying in these catalysts. It has been shown extensively that alloyed Au-Pd NPs are more active than monometallic NPs [5], and experimental studies combined with DFT calculations support the conclusion that the high reactivity of the smallest Au and Pd NPs is due to the abundance of low-coordinated atoms on the surfaces of these NPs [36,44].

4. Conclusion

This work has demonstrated that the catalytic activity of Au-Pd/Ti-NT catalysts in the selective oxidation of alcohols is strongly dependent on the catalyst preparation method, and that sol-immobilization is the most effective method for the preparation of Au-Pd/Ti-NT. The use of graphene oxide as stabilizer of the NPs appears promising. It is noteworthy to highlight that no attempt has been made in the current study to optimize the ratio of GO/(Au + Pd).

The present paper also elucidated the role of sodium and chlorides in the preparation of Au-Pd/Ti-NT by the adsorption method using $HAuCl_4.3H_2O$ and $PdCl_2$. The uptake of Pd ions from the aqueous solution was found to be dependent on the sodium content in Ti-NT. The concentration of Cl^- was found to affect the adsorption of the gold precursor by the Ti-NT support.

Characterization (XRD, TEM and XPS) and the catalytic activity tests indicate that the catalyst preparation method influences the activity by impacting strongly the size of the metal NP, the extent of alloy formation, and the location of the metal NPs with respect to the Ti-NT support.

Lastly, although there have been a few studies in literature on the influence of the catalyst preparation method on the activity of Au-Pd catalysts [3], this is the first study for Ti-NT supported catalysts. Indeed, the current study shows that the influence of the catalyst preparation on the activity is more pronounced and complex for Ti-NT than for conventional metal oxide supports (e.g. TiO_2, SiO_2,…etc.), due to the unique physiochemical properties of Ti-NT. The presence of cavities, the tube-like morphology, and ion-exchange characteristics of Ti-NT are among the many factors that profoundly influence the effectiveness of the catalyst preparation method and therefore the catalytic activity of Ti-NT-supported catalysts.

Acknowledgments

Motaz Khawaji gratefully acknowledges the financial support of Saudi Aramco. This work was funded in part by Saudi Aramco and EPSRC (EP/K014749/1). We are grateful to Dr. Ecaterina Ware for her assistance with TEM.

References

[1] D.I. Enache, J.K. Edwards, P. Landon, B. Solsona-Espriu, A.F. Carley, A.A. Herzing, M. Watanabe, C.J. Kiely, D.W. Knight, G.J. Hutchings, Solvent-free oxidation of primary alcohols to aldehydes using Au-Pd/TiO2 catalysts, Science 311 (2006) 362–365.
[2] Y.Y. Wu, N.A. Mashayekhi, H.H. Kung, Au–metal oxide support interface as catalytic active sites, Catal. Sci. Technol. 3 (2013) 2881.
[3] N. Dimitratos, A. Villa, C.L. Bianchi, L. Prati, M. Makkee, Gold on titania: effect of preparation method in the liquid phase oxidation, Appl. Catal. A: Gen. 311 (2006) 185–192.
[4] M. Haruta, Size- and support-dependency in the catalysis of gold, Catal. Today 36 (1997) 153–166.
[5] A. Villa, D. Wang, D.S. Su, L. Prati, New challenges in gold catalysis: bimetallic systems, Catal. Sci. Technol. 5 (2015) 55–68.
[6] C. Baatz, N. Decker, U. Pruse, New innovative gold catalysts prepared by an improved incipient wetness method, J. Catal. 258 (2008) 165–169.
[7] M. Sankar, Q. He, M. Morad, J. Pritchard, S.J. Freakley, J.K. Edwards, S.H. Taylor, D.J. Morgan, A.F. Carley, D.W. Knight, C.J. Kiely, G.J. Hutchings, Synthesis of stable ligand-free gold–palladium nanoparticles using a simple excess anion method, ACS Nano 6 (2012) 6600–6613.
[8] M. Okumura, S. Nakamura, S. Tsubota, T. Nakamura, M. Azuma, M. Haruta, Chemical vapor deposition of gold on Al2O3, SiO2, and TiO2 for the oxidation of CO and of H2, Catal. Lett. 51 (1998) 53–58.
[9] N. Dimitratos, J.A. Lopez-Sanchez, D. Morgan, A. Carley, L. Prati, G.J. Hutchings, Solvent free liquid phase oxidation of benzyl alcohol using Au supported catalysts prepared using a sol immobilization technique, Catal. Today 122 (2007) 317–324.
[10] D.V. Bavykin, A.A. Lapkin, P.K. Plucinski, L. Torrente-Murciano, J.M. Friedrich, F.C. Walsh, Deposition of Pt, Pd, Ru and Au on the surfaces of titanate nanotubes, Top. Catal. 39 (2006) 151–160.
[11] Á. Kukovecz, K. Kordás, J. Kiss, Z. Kónya, Atomic scale characterization and surface chemistry of metal modified titanate nanotubes and nanowires, Surf. Sci. Rep. 71 (2016) 473–546.
[12] L. Torrente-Murciano, T. Villager, D. Chadwick, Selective oxidation of salicylic alcohol to aldehyde with O2/H2using Au-Pd on titanate nanotubes catalysts, ChemCatChem 7 (2015) 925–927.
[13] M. Khawaji, D. Chadwick, Au-Pd bimetallic nanoparticles immobilised on titanate nanotubes: a highly active catalyst for selective oxidation, ChemCatChem 9 (2017) 4353–4363.
[14] R. Mueller, H.K. Kammler, K. Wegner, S.E. Pratsinis, OH surface density of SiO2 and TiO2 by thermogravimetric analysis, Langmuir 19 (2003) 160–165.
[15] D.V. Bavykin, F.C. Walsh, Titanate and Titania Nanotubes: Synthesis, Properties and Applications, (2009).
[16] A. Villa, D. Wang, G.M. Veith, F. Vindigni, L. Prati, Sol immobilization technique: a delicate balance between activity, selectivity and stability of gold catalysts, Catal. Sci. Technol. 3 (2013) 3036.
[17] T. Kasuga, M. Hiramatsu, A. Hoson, T. Sekino, K. Niihara, Formation of titanium

oxide nanotube, Langmuir 14 (1998) 3160–3163.
[18] N. Dimitratos, J.A. Lopez-Sanchez, D. Morgan, A.F. Carley, R. Tiruvalam, C.J. Kiely, D. Bethell, G.J. Hutchings, Solvent-free oxidation of benzyl alcohol using Au-Pd catalysts prepared by sol immobilisation, Phys. Chem. Chem. Phys. 11 (2009) 5142–5153.
[19] L. Torrente-Murciano, A.A. Lapkin, D. Chadwick, Synthesis of high aspect ratio titanate nanotubes, J. Mater. Chem. 20 (2010) 6484.
[20] R.A. Ortega-Domínguez, J.A. Mendoza-Nieto, P. Hernández-Hipólito, F. Garrido-Sánchez, J. Escobar-Aguilar, S.A.I. Barri, D. Chadwick, T.E. Klimova, Influence of Na content on behavior of NiMo catalysts supported on titania nanotubes in hydrodesulfurization, J. Catal. 329 (2015) 457–470.
[21] D.L. Morgan, H.-Y. Zhu, R.L. Frost, E.R. Waclawik, Determination of a morphological phase diagram of titania/titanate nanostructures from alkaline hydrothermal treatment of degussa P25, Chem. Mater. 20 (2008) 3800–3802.
[22] E. Morgado, M.A.S. de Abreu, G.T. Moure, B.A. Marinkovic, P.M. Jardim, A.S. Araujo, Characterization of nanostructured titanates obtained by alkali treatment of TiO2-anatases with distinct crystal sizes, Chem. Mater. 19 (2007) 665–676.
[23] E. Morgado, M.A.S. de Abreu, O.R.C. Pravia, B.A. Marinkovic, P.M. Jardim, F.C. Rizzo, A.S. Araújo, A study on the structure and thermal stability of titanate nanotubes as a function of sodium content, Solid State Sci. 8 (2006) 888–900.
[24] S. Ivanova, C. Petit, V. Pitchon, A new preparation method for the formation of gold nanoparticles on an oxide support, Appl. Catal. A: Gen. 267 (2004) 191–201.
[25] C. Baatz, N. Decker, U. Prüße, New innovative gold catalysts prepared by an improved incipient wetness method, J. Catal. 258 (2008) 165–169.
[26] L. Song, L. Cao, J. Li, W. Liu, F. Zhang, L. Zhu, G. Su, Lead titanate nanotubes synthesized via ion-exchange method: characteristics and formation mechanism, J. Alloys. Compd. 509 (2011) 6061–6066.
[27] D.V. Bavykin, K.E. Redmond, B.P. Nias, A.N. Kulak, F.C. Walsh, The effect of ionic charge on the adsorption of organic dyes onto titanate nanotubes, Aust. J. Chem. 63 (2010) 270–275.
[28] V. Bem, M.C. Neves, M.R. Nunes, A.J. Silvestre, O.C. Monteiro, Influence of the sodium/proton replacement on the structural, morphological and photocatalytic properties of titanate nanotubes, J. Photochem. Photobiol. A: Chem. 232 (2012) 50–56.
[29] L. Prati, A. Villa, Gold colloids: from quasi-homogeneous to heterogeneous catalytic systems, Acc. Chem. Res. 47 (2014) 855–863.
[30] N. Dimitratos, F. Porta, L. Prati, Au, Pd (mono and bimetallic) catalysts supported on graphite using the immobilisation method: synthesis and catalytic testing for liquid phase oxidation of glycerol, Appl. Catal. A: Gen. 291 (2005) 210–214.
[31] M. Khawaji, D. Chadwick, Au-Pd NPs immobilised on nanostructured ceria and titania: impact of support morphology on the catalytic activity for selective oxidation, Catal. Sci. Technol. (2018).
[32] D.R. Dreyer, S. Park, C.W. Bielawski, R.S. Ruoff, The chemistry of graphene oxide, Chem. Soc. Rev. 39 (2010) 228–240.
[33] L.J. Cote, J. Kim, Z. Zhang, C. Sun, J. Huang, Tunable assembly of graphene oxide surfactant sheets: wrinkles, overlaps and impacts on thin film properties, Soft Matter 6 (2010) 6096–6101.
[34] J. Wang, S.A. Kondrat, Y. Wang, G.L. Brett, C. Giles, J.K. Bartley, L. Lu, Q. Liu, C.J. Kiely, G.J. Hutchings, Au–Pd nanoparticles dispersed on composite titania/graphene oxide-supports as a highly active oxidation catalyst, ACS Catal. 5 (2015) 3575–3587.
[35] L. Torrente-Murciano, Q. He, G.J. Hutchings, C.J. Kiely, D. Chadwick, Enhanced Au-Pd activity in the direct synthesis of hydrogen peroxide using nanostructured titanate nanotube supports, ChemCatChem 6 (2014) 2531–2534.
[36] K. Mori, T. Hara, T. Mizugaki, K. Ebitani, K. Kaneda, Hydroxyapatite-supported palladium nanoclusters: a highly active heterogeneous catalyst for selective oxidation of alcohols by use of molecular oxygen, J. Am. Chem. Soc. 126 (2004) 10657–10666.
[37] B. Pawelec, A.M. Venezia, V. La Parola, E. Cano-Serrano, J.M. Campos-Martin, J.L.G. Fierro, AuPd alloy formation in Au-Pd/Al2O3 catalysts and its role on aromatics hydrogenation, Appl. Surf. Sci. 242 (2005) 380–391.
[38] C.W. Yi, K. Luo, T. Wei, D.W. Goodman, The composition and structure of Pd − Au surfaces, J. Phys. Chem. B 109 (2005) 18535–18540.
[39] B. Pawelec, A.M. Venezia, V. La Parola, E. Cano-Serrano, J.M. Campos-Martin, J.L.G. Fierro, AuPd alloy formation in Au-Pd/Al2O3 catalysts and its role on aromatics hydrogenation, Appl. Surf. Sci. 242 (2005) 380–391.
[40] Y.-F. Han, Z. Zhong, K. Ramesh, F. Chen, L. Chen, T. White, Q. Tay, S.N. Yaakub, Z. Wang, Au promotional effects on the synthesis of H2O2 directly from H2 and O2 on supported Pd − Au alloy catalysts, J. Phys. Chem. C 111 (2007) 8410–8413.
[41] S. Marx, A. Baiker, Beneficial interaction of gold and palladium in bimetallic catalysts for the selective oxidation of benzyl alcohol, J. Phys. Chem. C 113 (2009) 6191–6201.
[42] J. Pritchard, L. Kesavan, M. Piccinini, Q. He, R. Tiruvalam, N. Dimitratos, J.A. Lopez-Sanchez, A.F. Carley, J.K. Edwards, C.J. Kiely, G.J. Hutchings, Direct synthesis of hydrogen peroxide and benzyl alcohol oxidation using Au − Pd catalysts prepared by sol immobilization, Langmuir 26 (2010) 16568–16577.
[43] M. Khawaji, D. Chadwick, Au–Pd NPs immobilised on nanostructured ceria and titania: impact of support morphology on the catalytic activity for selective oxidation, Catal. Sci. Technol. 8 (2018) 2529–2539.
[44] B. Hvolbæk, T.V.W. Janssens, B.S. Clausen, H. Falsig, C.H. Christensen, J.K. Nørskov, Catalytic activity of Au nanoparticles, Nano Today 2 (2007) 14–18.